Acta Crystallographica Section B
Structural Science
ISSN 0108-7681

Proton-transfer dynamics in the $(HCO_3^-)_2$ dimer of $KHCO_3$ from Car–Parrinello and path-integrals molecular dynamics calculations

Przemyslaw D. Dopieralski,[a]* Zdzislaw Latajka[a] and Ivar Olovsson[b]

[a]University of Wroclaw, Faculty of Chemistry, 14 Joliot-Curie Str. 50-383 Wroclaw, Poland, and [b]Department of Materials Chemistry, Ångström Laboratory, SE-751 21 Uppsala, Sweden

Correspondence e-mail: mclar@elrond.chem.uni.wroc.pl

Received 1 December 2009
Accepted 18 January 2010

The proton motion in the $(HCO_3^-)_2$ dimer of $KHCO_3$ at 298 K has been studied with Car–Parrinello molecular dynamics (CPMD) and path-integrals molecular dynamics (PIMD) simulations. According to earlier neutron diffraction studies at 298 K hydrogen is disordered and occupies two positions with an occupancy ratio of 0.804/0.196. A simulation with only one unit cell is not sufficient to reproduce the disorder of the protons found in the experiments. The CPMD results with four cells, 0.783/0.217, are in close agreement with experiment. The motion of the two protons along the O···O bridge is highly correlated inside one dimer, but strongly uncoupled between different dimers. The present results support a mechanism for the disorder which involves proton transfer from donor to acceptor and not orientational disordering of the entire dimer. The question of simultaneous or successive proton transfer in the two hydrogen bonds in the dimer remains unanswered. During the simulation situations with almost simultaneous proton transfer with a time gap of around 1 fs were observed, as well as successive processes where first one proton is transferred and then the second one with a time gap of around 20 fs. The calculated vibrational spectrum is in good agreement with the experimental IR spectrum, but a slightly different assignment of the bands is indicated by the present simulations.

1. Introduction

Proton transfer between donor and acceptor in hydrogen bonds is one of the simplest chemical reactions and plays an important role in many fields of physics, chemistry and life sciences (Pauling, 1960; Schuster *et al.*, 1976, Schuster, 1984; Jeffrey & Saenger, 1991; Scheiner, 1997). For instance, most biological processes involve forming and breaking hydrogen bonds and proton transfer is an important step in this context. Potassium hydrogen carbonate ($KHCO_3$) is a perfect model system to study proton-transfer dynamics in the solid state. The crystal structure has been studied in detail by X-ray and neutron diffraction by Thomas *et al.* (1974*a*,*b*); *cf.* earlier studies by Nitta *et al.* (1952, 1954) and Pedersen (1968). The structure contains centrosymmetric carboxylate dimers $(HCO_3)_2^{2-}$ with moderately strong O···O hydrogen bonds (2.59 Å) and with disordered proton distribution. The dynamics of the protons have been investigated with many different techniques and theoretical methods: NMR (Benz *et al.*, 1986; Odin, 2004), quasi-elastic neutron scattering (Eckold *et al.*, 1992) spectroscopy (Fillaux, 1983, 2000; Brierley *et al.*, 1978), static theoretical calculations (Wójcik *et al.*, 2002) and *ab initio* and molecular dynamics simulations (Dopieralski, Latajka & Olovsson, 2009).

Neutron diffraction studies of $KHCO_3$ and $KDCO_3$ by Thomas *et al.* (1974*b*) showed that at 298 K the H and D atoms are disordered over two sites with an occupancy ratio of 0.804/0.196 for H and 0.877/0.123 for D. According to the neutron diffraction studies by Fillaux *et al.* (2003, 2006) the H atom occupies a single position at low temperature (14 and 150 K). Fillaux *et al.* (2006) report for H an occupancy ratio at 200 K equal to 0.959/0.041 and at 300 K equal to 0.823/0.177. Sugiyama *et al.* (1998) report an occupancy ratio of 0.668/0.332 for D at 345 K, and in the high-temperature phase (363 K) an occupancy ratio for D of 0.50/0.50. The source of the disorder has been much debated. A fundamental question is whether there is a static or dynamic disorder of the proton distribution. Is there an orientational disordering of the entire $(HCO_3)_2^{2-}$ dimer, or do the two protons in the dimer jump across the hydrogen bonds – simultaneously or independent of each other? In an attempt to answer some of these questions molecular dynamics simulations have been made to determine the motion and the occupancy ratio of the proton positions in the dimer. Our studies involve the crystal structure at 298 K. The crystal is monoclinic, space group $P2_1/a$ (equivalent to $P2_1/c$) with four formula units ($Z = 4$) in a unit cell with dimensions $a = 15.1725$, $b = 5.6283$ and $c = 3.7110$ Å and $\beta = 104.63^\circ$ (Thomas *et al.* (1974*a*). The crystal structure parameters at 298 K were used as starting parameters in both the CPMD and PIMD simulations.

In our previous preliminary report (Dopieralski, Latajka & Olovsson, 2009) it was shown that *ab initio* molecular-dynamics simulations are able to reproduce the experimentally determined proton occupancy ratio very well. Our study involved the introduction of an enlarged simulation model with the periodic boundary condition (PBC) and with a four-crystal cell model (4C) instead of *k*-points sampling. The 4C model was introduced to obtain a more correct description of the dynamical situation in the crystal. In the present paper we discuss in more detail the proton motion as well as the time gap between proton jumps and proton correlations. The simulated vibrational spectrum is compared with the experimental spectrum to investigate whether the 4C approximation is good enough to reproduce not only the occupancy ratio but also the vibrational spectrum.

2. Method

Two types of molecular-dynamics simulations were carried out. In the first, the behaviour of all atoms was treated classically with the Car–Parrinello molecular dynamics (CPMD) method (Car & Parrinello, 1985) using Version 3.11.1 (CPMD, 1990–2008). In the second, the path-integrals molecular dynamics (PIMD) method was applied (Marx & Parrinello, 1994, 1996; Tuckerman *et al.*, 1996). Within the PIMD approach it is possible to obtain a much more reliable description of nuclear motion due to the quantum effects incorporated in the model. In the PIMD method the nuclei are treated as quantum particles.

In the first calculations the simulations were performed with one crystal unit cell (1C) and with periodic boundary conditions (PBC). Following the initial equilibrium period (*ca* 20 000 steps), data were collected over trajectories spanning 1 000 000 steps (more than 60 ps) for the Car–Parrinello dynamics and 600 000 steps (more that 40 ps) for path-integrals dynamics. Additionally, calculations were carried out with a larger fragment of the crystal with 4 unit cells (4C model) and simulations were run up to 500 000 steps (around 35 ps) for the Car–Parrinello dynamics and 120 000 steps (around 9 ps) for the path-integrals dynamics method. Owing to the very time-consuming calculation we are not able to reach equilibrium in the PIMD approach with the 4C model. The 9 ps run with PIMD was at least as expensive as the 35 ps run with CPMD. We have decided to present the PIMD results mainly to show that in this particular case PIMD does not provide convergence of the occupancy ratio faster than the CPMD approach, but is associated with considerably larger costs. In the PIMD simulations 8 beads and the normal-mode variable transformation were used (Tuckerman *et al.*, 1996). Our previous results on the fumaric acid crystal (Dopieralski, Panek & Latajka, 2009) demonstrated that the 8 beads approximation was sufficient for the studied system and is a satisfactory compromise between reliable results and reasonable computer time. A kinetic energy cutoff of 100 Ry was used for the electron plane-wave basis; Troullier & Martins (1991) pseudopotentials and PBE exchange and correlation functionals (Perdew *et al.*, 1996) were applied. To control the temperature of the system the Nose–Hoover-chain thermostat (Nose, 1984; Martyna *et al.*, 1992) was turned on and set at the frequency 3000 cm^{-1}. The fictitious kinetic energy of the orbitals was controlled in each separate simulation. For the PIMD simulations, a separate thermostat was used for each degree of freedom (Tuckerman, 2002). The time step was equal to 3 a.u. We have adopted the same approach as Miura *et al.* (1998) in which the positions of the atoms evolve according to the classical equation of motion. The PIMD simulation explores the quantum behaviour of both the nuclear and electronic degrees of freedom. It maps the problem of a quantum particle into one of a classical ring polymer model with beads that interact through temperature and mass-dependent spring forces. In the literature it is known as a quantum-classical isomorphism (Feynman & Hibbs, 1965; Schweizer *et al.*, 1981; Chandler & Wolynes, 1981). It should be underlined that the 'real' properties of the quantum systems are recovered only when the number of beads reaches infinity. The free-energy profiles were obtained from the equation

$$\Delta F = -kT \ln[P(\delta)], \qquad (1)$$

where k = Boltzmann's constant, T = simulation temperature and $P(\delta)$ is the proton distribution as a function of δ, the reaction coordinate. The reaction coordinate is defined as the difference $\delta = r_{O-H} - r_{H\cdots O}$. The δ value is used as a measure of the proton-transfer degree in the hydrogen bond (zero on the reaction coordinate axis indicates the midpoint of the hydrogen bridge).

The occupancy ratio was obtained in each case (CPMD, PIMD) using the same routine, based on the distribution function obtained from the simulation. First the distribution

function was divided into two regions – below the reaction coordinate equal to zero, and above the reaction coordinate equal to zero. Then the profiles were integrated and obtained values were averaged over all eight dimers.

It should be pointed out that all the calculations were carried out with only a Γ-point approximation, but this approximation is well established if the simulation cell is large enough (Jezierska & Panek, 2009). *k*-points sampling with *ab initio* molecular dynamics is extremely expensive. Instead of *k*-points sampling the simulation cell was enlarged and a 4C model introduced to obtain a more correct description of the dynamical situation in the crystal (for more details see our previous paper Dopieralski, Latajka & Olovsson, 2009).

Vibrational spectra have been generated using a program written by Forbert (2002), which calculates the fast Fourier transform of the classical autocorrelation function of the total dipole moment, including all contributions – nuclear and electronic. The so-called high-temperature (or harmonic) quantum correction factors to the classical line-shape functions were used to approximate the true quantum line-shape function and thus the IR spectra (Ramirez *et al.*, 2004). This method is found to work well for anharmonic vibrational spectra and hydrogen-bonded systems (Asvany *et al.*, 2005; Mathias & Marx, 2007; Kumar & Marx, 2006; Rousseau *et al.*, 2004). The visual molecular dynamics (VMD; Humphrey *et al.*, 1996) program has been used for data visualization.

3. Results and discussion

Fig. 1 shows a three-dimensional representation of the locations of the atoms in the two O···O hydrogen bonds in one selected dimer, obtained from the CPMD and PIMD simulations with the 4C model. The left part corresponds to a static situation, and then shows isosurfaces at 100 K, where proton transfer was not observed. The third part illustrates the proton transfer at 298 K. The last part corresponds to full quantum treatment of the system (8 beads approximation). The positions of the atoms are more diffuse in this study compared with the CPMD method.

The correlation of the reaction coordinates inside one selected dimer is shown in Fig. 2 (the same situation was observed in all dimers) and the correlation of reaction coordinates from different dimers in Fig. 3. From Fig. 2 we notice that the motion of the two protons along the O···O bridge is highly correlated inside one dimer. Additionally Fig. 2 is proof that during simulations protons inside one dimer cannot jump over the barrier independent of each other. The conclusion is that the mechanism of double proton transfer over the barrier inside one dimer cannot be described as purely simultaneous or successive – in most cases situations in between these two are observed. In contrast, the proton motion in different dimers is strongly uncoupled, as illustrated in Fig. 3. The absence of points around the middle of the picture, where both reaction coordinates are equal to zero, suggests that protons from different dimers do not transfer at the same time (*cf* blue arrows).

To study the details of the proton transfer within one selected dimer we performed a procedure similar to that used by Ushiyama & Takatsuka (2001) to define the relative coordinates of the protons in the dimer. The first parameter, n_1, is the projection of the O—H distance in the O···O direction divided by the O···O distance for the first hydrogen bond in the selected dimer. The second parameter, n_2, is the corresponding parameter for the second

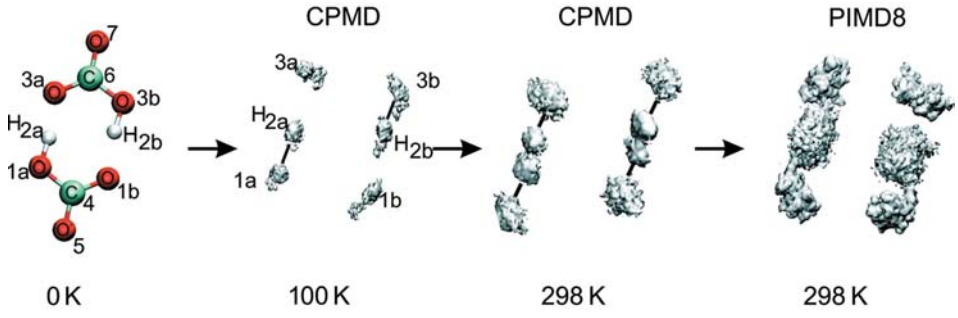

Figure 1
Three-dimensional isosurfaces at different temperatures for one selected dimer of $(HCO_3^-)_2$ from CPMD and PIMD(8) simulations; all with PBC included and with the 4 unit-cell model.

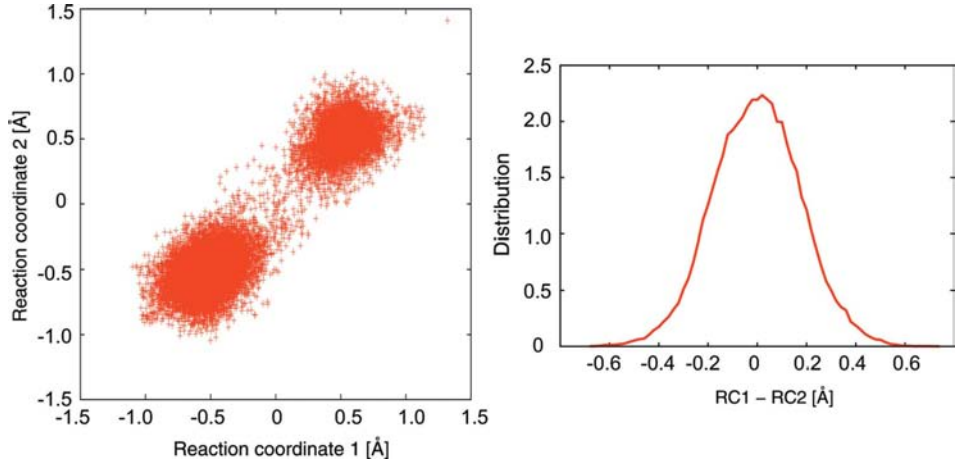

Figure 2
The left picture shows the correlation between the two reaction coordinates inside one selected dimer of $(HCO_3^-)_2$. The right picture shows the distribution of the difference of the reaction coordinates for one selected dimer (CPMD results).

hydrogen bond in the selected dimer. Fig. 4 shows four selected proton jumps in the new set of parameters n_1 and n_2. Only the most representative situations have been illustrated. During the simulation situations with almost simultaneous proton transfer were observed, with a time gap between the proton transfer in the two hydrogen bonds of 1 fs (*cf.* Fig. 4*a*), as well as successive processes where first one proton is transferred and then the second one, with a time gap around 20 fs (Fig. 4*c*). Also a situation where one proton is moving to the middle of the hydrogen bond and oscillates there for a few fs waiting for a second proton was observed (Fig. 4*b*). When the second proton reaches the middle of the hydrogen bond then both of them are transferred. The last picture (Fig. 4*d*) corresponds to a case where both protons oscillate around the middle of the hydrogen bond. These four selected situations are clear evidence that proton transfer cannot be described as a pure simultaneous or successive process. There is a strong coupling between the O—H and O···O motion and as a consequence of that we found that proton transfer occurs only when the O···O distance is shorter than the distance observed in the optimized structure – usually less than 2.5 Å.

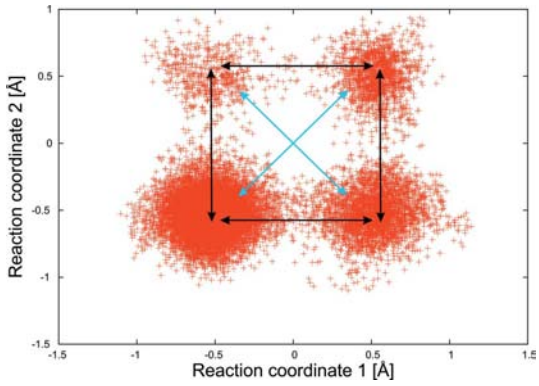

Figure 3
Correlation of reaction coordinates between two different dimers of $(HCO_3^-)_2$ (arbitrary selection of one of the two reaction coordinates for either dimer; all situations give smilar plots; CPMD results). Black arrows show how the proton transfers occur; blue arrows represent the case when both protons from different dimers are transferring at the same time – this situation is not observed in the simulations (there are no points around the middle of the picture).

During the 35 ps simulations 10, 6, 10, 4, 6, 6 10 and 11 jumps were observed in the different dimers. The average is around eight jumps per dimer during the 35 ps run. Statistically we thus observed one proton transfer every 4 ps. When we take the proton jumps in all four unit cells into account, 63 jumps over 35 ps were observed – almost two reactions per picosecond. When the time lag between proton transfers is considered, the order for one selected dimer was as follows: 2, 10, 10, 2, 5, 8, 6, 17, 6 and 7 fs. For the next dimer it was 12, 1, 7, 6, 8 and 10 fs. The remaining dimers had similar timings. To trace which one of the two protons within one dimer starts the reaction, we marked them as H1 and H2. Thus, the order of protons undergoing transfer looks like this: H2 H2 H1 H2 H2 H1 H1 H1 H1 H1.

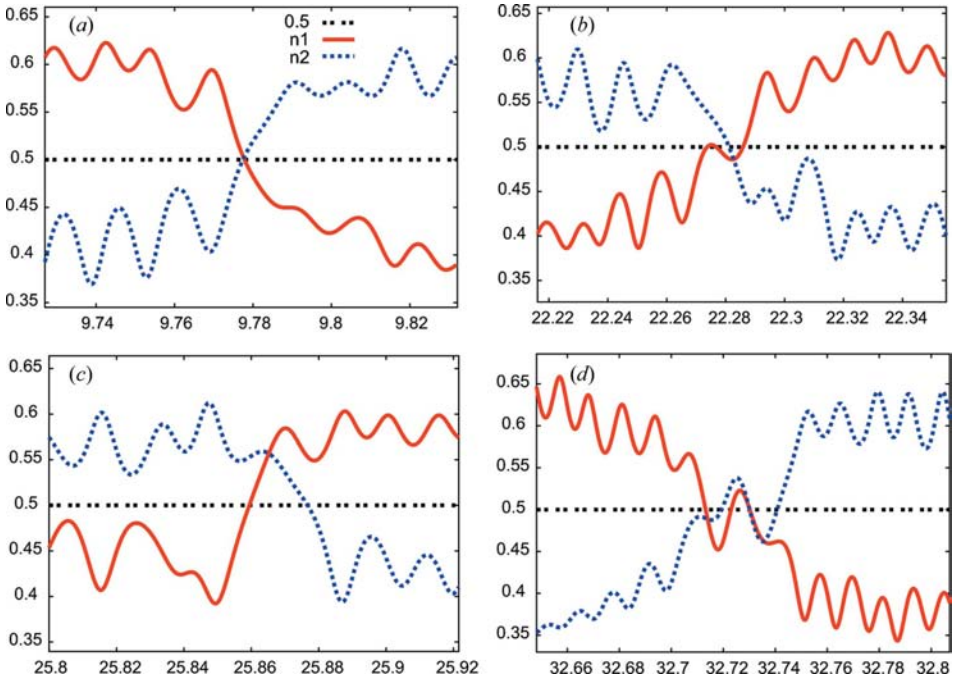

Figure 4
Four selected protons jumps (CPMD results at 298 K). On the vertical axis are n_1 and n_2 coordinates and on the horizontal axis time in ps. Picture (*a*) shows an almost simultaneous proton transfer, and (*b*) oscillation of one proton (red curve) around the middle of the hydrogen bond. Picture (*c*) shows a situation close to successive proton transfer. Picture (*d*) shows a situation where both protons oscillate around the middle of the hydrogen bond.

In Fig. 5 the new coordinate r_1 is the sum of two reaction coordinates from one selected dimer, whereas variable r_2 is the sum of two O···O distances in the same dimer. From Fig. 5 we observe that proton transfer occurs only when the O···O distance (variable r_2 divided by 2) is much shorter than the distance in the optimized structure. Proton transfer occurs when the sum of the two O···O distances is in the range 4.6–5.0 Å. This means that each O···O distance is around 2.3–2.5 Å, which is a very short hydrogen bridge.

The proton-distribution functions are presented in Fig. 6. It is important to note that for the 1C model system with PBC only one maximum at $\delta = -0.68$ Å is observed with the CPMD simulation, as well as one at $\delta = -0.66$ Å with the quantum simulation (PIMD). The results for the 1C model clearly indicate a lack of proton transfer in the dimer. A completely different picture is

Table 1
Bands observed in the spectra obtained from CPMD simulation compared with experiment.

Band (cm^{-1})	CPMD 1C	CPMD 4C	Expt. (KBr) [sdbs]	Expt. (Nakamoto *et al.*, 1965)	Expt. 5 K (Fillaux *et al.*, 1988)
ν(O—H)	3370–2500	3180–1800	3500–2100	2920, 2620	3500–1800
ν(C═O) + ν(C—O^-)	1608 1589, 1619, 1630	1530 1519, 1542, 1561	1631 1657, 1650	1650, 1618	
ν(C═O) + ν(C—O) + ν(C—O^-) + δ (OHO)	1350	 1310 1330, 1360	 1403 1372	1367, 1405 ν(C—O) + ν(C—O^-) + δ(OHO)	1400 δ(OHO)
ν(C═O) + ν(C—O) + ν(C—O^-) + γ(OH)	995	994 945	1008 982	1001 988 γ(OHO)	983 γ(OH) 933 γ(OH)
	782	778 775	834	830 $\pi(CO_3)$	
	646	657 622	703 663	698 655 δ(OCO)	639 $\gamma(CO_3)$ 621 $\gamma(CO_3)$
ν(O···O)	205–50	153 127		248 ν(O···H) + δ(C═O) 186 Ring def.	225 ν(O···O) 219 ν(O···O)

obtained from calculations with the four cells (4C) approximation and with PBC included. As seen in Fig. 6, two maxima appear at $\delta = -0.54$ and +0.54 Å, with the CPMD simulation. Including four cells (4C) in the simulations evidently changes the behavior of the protons. Simulation with only one unit cell (1C) is clearly not sufficient to reproduce the disorder of the protons found in the experiments. Even 'full' quantum treatment (PIMD8) with only one cell does not provide better results. When analyzing Fig. 6 it can be concluded that the population at $\delta = 0$ is larger for the quantum case (PIMD) than for CPMD. This indicates that we have an increase in frequency of proton transfers in the PIMD case in comparison to CPMD. A short CPMD simulation of 10 ps with the 4C model performed at 100 K indicated that this is too low a temperature to push the protons across the energy barrier.

The results from the 4C CPMD model simulations are in very good agreement with experimental data. The simulations from the 35 ps period reproduce experimental bond lengths within +0.06 Å in the worst case (compared with the experimental values involving hydrogen from the neutron study, *cf.* Dopieralski *et al.*, 2009). In all the simulations only 4C reproduces the O···O distance exactly. As seen from Fig. 6 simulations for the 1C system do not predict any proton transfer as a possible mechanism for the disorder of the protons. Finally, molecular dynamics for the 4C system demonstrate that the situation reported by Thomas *et al.* (1974*a*,*b*), with disordered protons and an occupancy ratio of about 0.804/0.196, is possible with a mechanism involving proton transfer. The occupancy ratio derived from the present calculations, 0.783/0.217, reproduces the experimental value with an accuracy of $\pm$ 0.02 after the 35 ps run (the average for eight hydrogen bonds with the 4C model, Fig. 7); *cf.* the relative occupancy of the disordered protons illustrated in Fig. 1. Orientational disordering of the entire $(HCO_3^-)_2$ is not excluded, but in the light of our study is less probable. Additionally we have shown in Fig. 7 the PIMD results, which illustrate that PIMD does not result in convergence of the occupancy ratio faster than CPMD. It also shows

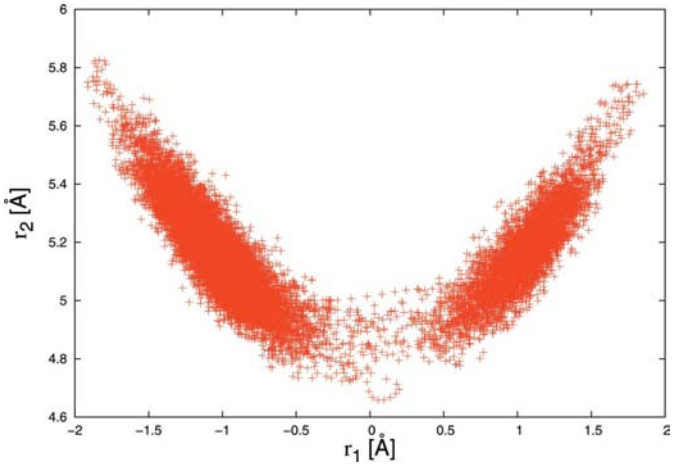

Figure 5
Correlation of r_1 (sum of two reaction coordinates) and r_2 (sum of two O···O distances) inside one dimer (CPMD results).

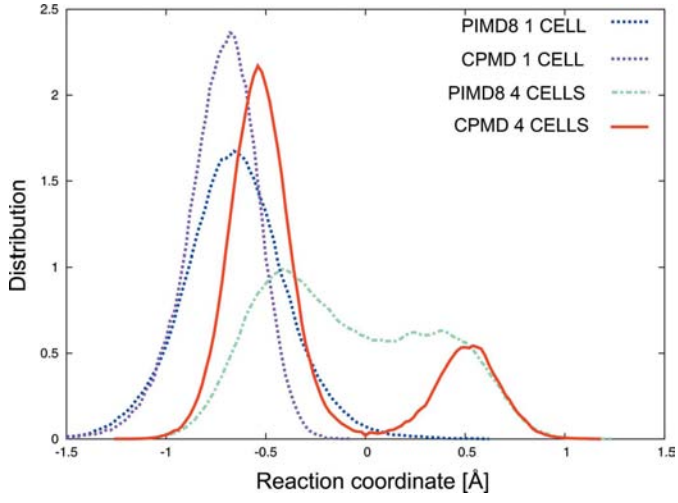

Figure 6
Distribution function of the protons at 298 K. Dark blue curve: one cell with full quantum dynamics – path integrals simulation with 8 beads (PIMD8); purple curve: one cell with Car–Parrinello simulation; light blue curve: four cells with PIMD8; red curve: four cells with Car–Parrinello simulation. All simulations with PBC.

that the PIMD results follow the CPMD results. The conclusion is that it is not necessary to use a sophisticated method like PIMD to determine the occupancy ratio. However, the situation could be different for systems where quantum effects play a crucial role.

Previous findings by INS (inelastic neutron scattering; Fillaux *et al.*, 1988) indicate that the proton dynamics are almost completely decoupled from those of the heavy atoms.

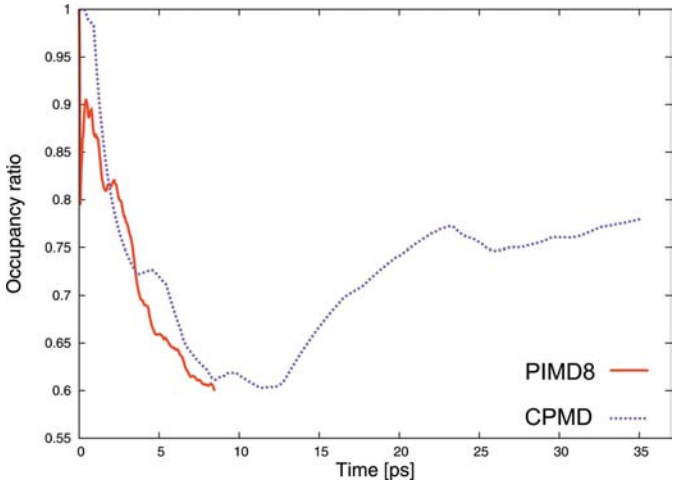

Figure 7
Average of the occupancy ratios for all eight hydrogen bonds; results for the 4C model for CPMD and PIMD simulation.

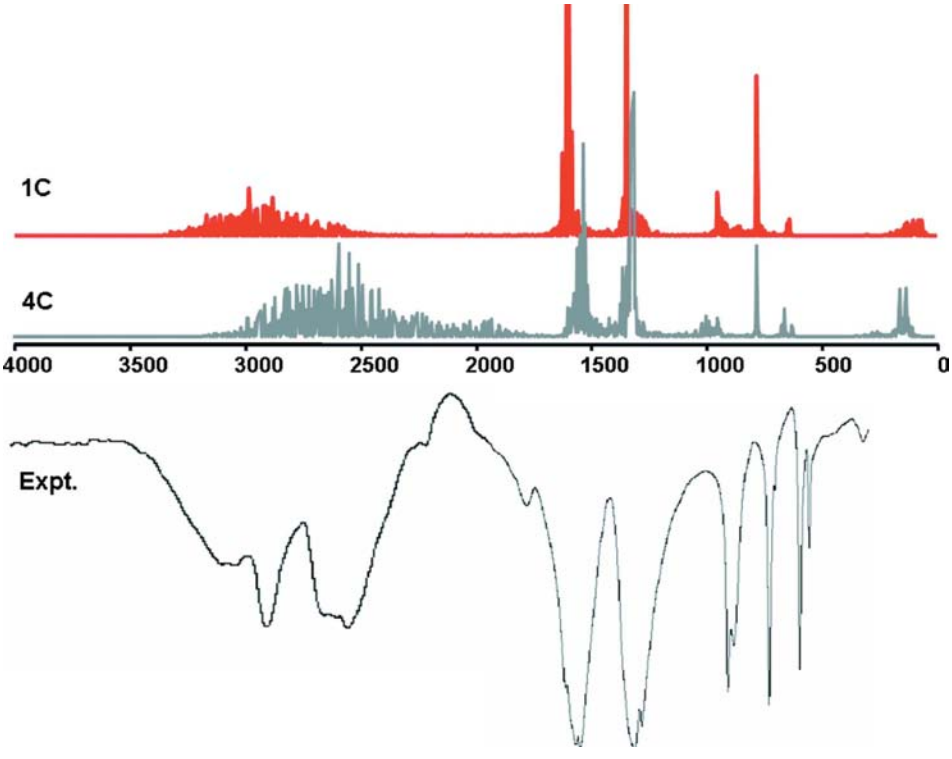

Figure 8
Comparison between theoretical and experimental spectra. Red curve CPMD simulation with 1C model (no proton transfer), grey curve with 4C model. Experimental IR spectrum taken from the SDBS database, KBr disk experiment. This figure is in colour in the electronic version of this paper.

This conclusion was also drawn in our previous CPMD study with fixed potassium positions (4C model; Dopieralski *et al.*, 2009). However, the proton position is expected to be highly correlated with the positions of the O atoms in the hydrogen bond. Also the two protons in the dimer are strongly correlated (Fig. 3).

4. Vibrational spectra

The proton dynamics in the quantum regime has been intensively studied with vibrational spectroscopy (Fillaux, 1983; Fillaux *et al.*, 1988, 2000; Novak *et al.*, 1963). In the IR and Raman spectra the O—H stretching vibration was observed as a broad band, with several submaxima between 3500 and 1800 cm^{-1}, which is in agreement with our CPMD study for the 4C model system. All theoretical and experimental spectra discussed here are IR. A comparison between the experimental and calculated spectra is shown in Fig. 8. The assignment of bands in the IR spectrum is presented in Table 1. When comparing the 1C and 4C model spectra we notice a broader band at 3180 to 1800 cm^{-1} for the 4C model due to the proton-transfer process. Also the bands observed for the 1C model at 1608 and 1350 cm^{-1} are now shifted to lower wavenumbers, 1530 and 1310 cm^{-1}. Additionally, splitting of some bands is observed when going from the 1C to the 4C model: the band at 995 cm^{-1} splits into two bands at 994 and 995 cm^{-1}; the bands at 782 and 646 cm^{-1} are split into bands at 778, 775 cm^{-1} and 657, 622 cm^{-1}, respectively. The broad absorption band at around 205–50 cm^{-1} for the 1C model is changed to a doublet at 153, 127 cm^{-1} for the 4C model.

5. Conclusions

Introduction of a 4C model with Γ-point approximation and with PBC is able to describe properly the proton dynamics in the hydrogen bonds and the experimental occupancy ratio is reproduced with high accuracy. The motion of the two protons along the O···O bridge is highly correlated inside one dimer of $(HCO_3^-)_2$. However, the strong and unrealistic coupling of the proton motion in different $(HCO_3^-)_2$ dimers introduced by the one unit-cell approximation (1C) does not correspond to the true behaviour of the protons. Examination of the dynamics of a larger part of the solid (4C model) results in decoupling of the proton motions in different $(HCO_3^-)_2$ dimers. The present

results support a mechanism for the disorder which involves proton transfer from donor to acceptor, but not orientational disordering of the entire $(HCO_3^-)_2$ dimer. Additionally we found that proton transfer occurs only when the O···O distance is shorter than the distance observed in the optimized structure, usually less than 2.5 Å. The question of simultaneous or successive proton transfer in the two hydrogen bonds in the dimer remains unanswered. The conclusion is that the proton-transfer mechanism cannot be described as strictly simultaneous or successive as situations close to both of these scenarios were observed. In the present CPMD simulations the observed time lag between proton transfers within one dimer is in the range 1–20 fs.

The authors gratefully acknowledge the Wroclaw Supercomputer Center (WCSS), the Galera-ACTION Cluster and the Academic Computer Center in Gdańsk (CI TASK) for providing the computer time. The authors thank the Ministry of Science and Higher Education of Poland (MNiSz) for funding under Grant No. N N204 0958 33. The authors also thank Professor Kersti Hermansson for fruitful discussion and comments.

References

Asvany, O., Kumar, P., Redlich, P. B., Hegemann, I., Schlemmer, S. & Marx, D. (2005). *Science*, **309**, 1219–1222.

Benz, S., Haeberlen, U. & Tegenfeldt, J. (1986). *J. Magn. Res.* **66**, 125.

Brierley, K. P., Howard, J., Ludmann, C. J., Robson, K., Waddington, T. C. & Tomkinson, J. (1978). *Chem. Phys. Lett.* **59**, 467–471.

Car, R. & Parrinello, M. (1985). *Phys. Rev. Lett.* **55**, 2471–2474.

Chandler, D. & Wolynes, P. G. (1981). *J. Chem. Phys.* **74**, 4078–4095.

CPMD (1990–2008). http://www.cpmd.Org/, Copyright IBM Corp, Copyright MPI für Festkörperforschung Stuttgart.

Dopieralski, P., Latajka, Z. & Olovsson, I. (2009). *Chem. Phys. Lett.* **476**, 223–226.

Dopieralski, P., Panek, J. & Latajka, Z. (2009). *J. Chem. Phys.* **130**, 164517–9.

Eckold, G., Grimm, H. & Stein-Arsic, M. (1992). *Physica B*, **180**, 336–338.

Feynman, R. P. & Hibbs, A. R. (1965). *Quantum Mechanics and Path Integrals*. New York: McGraw-Hill.

Fillaux, F. (1983). *Chem. Phys.* **74**, 405–412.

Fillaux, F. (2000). *Int. Rev. Phys. Chem.* **19**, 553–564.

Fillaux, F., Cousson, A. & Gutmann, M. J. (2006). *J. Phys. Condens. Matter*, **18**, 3229–3249.

Fillaux, F., Cousson, A. & Keen, D. (2003). *Phys. Rev. B*, **67**, 054301–10.

Fillaux, F., Tomkinson, J. & Penfold, J. (1988). *Chem. Phys.* **124**, 425–437.

Forbert, H. (2002). Local program, Version 30.04.2002. Ruhr University Bochum, Germany

Humphrey, W., Dalke, A. & Schulten, K. (1996). *J. Mol. Graph.* **12**, 33.

Jeffrey, G. A. & Saenger, W. (1991). *Hydrogen Bonding in Biological Structures*. Berlin: Springer-Verlag.

Jezierska, A. & Panek, J. J. (2009). *J. Comput. Chem.* **30**, 1241–1250.

Kumar, P. & Marx, D. (2006). *Phys. Chem. Chem. Phys.* **8**, 573–586.

Martyna, G. J., Tuckerman, M. & Klein, M. L. (1992). *J. Chem. Phys.* **97**, 2635–2643.

Marx, D. & Parrinello, M. (1994). *Z. Phys. B*, **95**, 143–144.

Marx, D. & Parrinello, M. (1996). *J. Chem. Phys.* **104**, 4077–4082.

Mathias, G. & Marx, D. (2007). *Proc. Natl. Acad. Sci. USA*, **104**, 6980–6985.

Miura, Y. S., Tuckerman, M. & Klein, M. L. (1998). *J. Chem. Phys.* **109**, 5290–5299.

Nakamoto, K., Anantarama Sarma, Y. & Ogoshi, H. (1965). *J. Chem. Phys.* **43**, 1177–1181.

Nitta, I., Tomiie, Y. & Koo, C. H. (1952). *Acta Cryst.* **5**, 292.

Nitta, I., Tomiie, Y. & Koo, C. H. (1954). *Acta Cryst.* **7**, 140–141.

Nose, S. (1984). *Mol. Phys.* **52**, 255–268.

Novak, A., Saumagne, P. & Bock, L. D. C. (1963). *J. Chim. Phys. Phys. Chim. Biol.* **60**, 1385–1394.

Odin, C. (2004). *J. Phys. Chem B*, **108**, 7402–7411.

Pauling, L. (1960). *The Nature of Chemical Bond*. Ithaca: Cornell University Press.

Pedersen, B. (1968). *Acta Cryst.* B**24**, 478–480.

Perdew, J. P., Burke, K. & Ernzerhof, M. (1996). *Phys. Rev. Lett.* **77**, 3865–3868.

Ramirez, R. P., Lopez-Ciudad, T., Kumar, P. & Marx, D. (2004). *J. Chem. Phys.* **121**, 3973–3984.

Rousseau, R., Kleinschmidt, V., Schmitt, U. W. & Marx, D. (2004). *Angew. Chem. Int. Ed.* **43**, 4804–4807.

Scheiner, S. (1997). *Hydrogen Bonding: A Theoretical Perspective.* Oxford University Press.

Schuster, P. (1984). *Hydrogen Bonds.* Berlin: Springer-Verlag.

Schuster, P., Zundel, G. & Sandorfy, C. (1976). Editors. *The Hydrogen Bond, Recent Developments in Theory and Experiments*, Vols. I–III. Amsterdam: North-Holland.

Schweizer, K. S., Stratt, R. M., Chandler, D. & Wolynes, P. G. (1981). *J. Chem. Phys.* **75**, 1347–1363.

Sugiyama, M., Machida, M., Hanashiro, K., Koyano, N. & Iwata, Y. (1998). *Physica B*, **241**, 367–369.

Thomas, J. O., Tellgren, R. & Olovsson, I. (1974*a*). *Acta Cryst.* B**30**, 1155–1166.

Thomas, J. O., Tellgren, R. & Olovsson, I. (1974*b*). *Acta Cryst.* B**30**, 2540–2549.

Troullier, N. & Martins, J. L. (1991). *Phys. Rev. B*, **43**, 1993–2006.

Tuckerman, M. (2002). *NIC Series*, **10**, 269–298.

Tuckerman, M., Marx, D., Klein, M. L. & Parrinello, M. (1996). *J. Chem. Phys.* **104**, 5579–5588.

Ushiyama, H. & Takatsuka, K. (2001). *J. Chem. Phys.* **115**, 5903–5912.

Wójcik, M. J., Tatara, W. & Ikeda, S. (2002). *J. Mol. Struct.* **614**, 109–115.